

Supersymmetry with scalar sequestering

Howard Baer^{1*}, Vernon Barger^{2†}, Dakotah Martinez^{1‡}

¹*Homer L. Dodge Department of Physics and Astronomy,
University of Oklahoma, Norman, OK 73019, USA*

²*Department of Physics, University of Wisconsin, Madison, WI 53706 USA*

Abstract

Supersymmetric models with a strongly interacting superconformal hidden sector (HS) may drive soft SUSY breaking scalar masses, bilinear soft term $B\mu$ and Higgs combinations $m_{H_{u,d}}^2 + \mu^2$ to small values at some intermediate scale, leading to unique sparticle mass spectra along with possibly diminished finetuning in spite of a large superpotential μ parameter. We set up a computer code to calculate such spectra, which are then susceptible to a variety of constraints: 1. possible charge-or-color breaking (CCB) minima in the scalar potential, 2. unbounded from below (UFB) scalar potential, 3. improper electroweak symmetry breaking, 4. a charged or sneutrino lightest SUSY particle (LSP), 5. generating $m_h \sim 125$ GeV, 6. consistency with LHC sparticle mass limits, and 7. naturalness. We find this bevy of constraints leaves little or no viable parameter space for the case where hidden sector dynamics dominates MSSM running, even for the case of non-universal gaugino masses. For the case with moderate HS running with comparable MSSM running, and with universal gaugino masses, then the finetuning is ameliorated, but nonetheless remains high. Viable spectra with moderate HS running and with low finetuning and large μ can be found for non-universal gaugino masses.

*Email: baer@ou.edu

†Email: barger@pheno.wisc.edu

‡Email: dakotah.s.martinez-1@ou.edu

1 Introduction

Particle physics models featuring weak scale supersymmetry [1, 2] (SUSY) are notable in that they contain a solution to the gauge hierarchy problem (GHP) and are supported by several virtual effects, including the celebrated unification of gauge couplings, a prediction for the Higgs mass within expectations from theory and experiment, and a prediction of a heavy top quark needed for radiative electroweak symmetry breaking (EWSB) well before the top quark was discovered. Even so, the non-appearance of supersymmetric matter at the CERN Large Hadron Collider [3] (LHC) has potentially opened up a different naturalness problem [4]: the little hierarchy problem (LHP) concerning the burgeoning mass gap between the weak scale $m_{weak} \sim m_{W,Z,h} \sim 100$ GeV and the so-called soft SUSY breaking scale $m_{soft} \sim m_{sparticles}$, *i.e.* why is $m_{weak} \ll m_{soft} \gtrsim 1 - 10$ TeV?

A potential solution to the LHP comes from examining the explicit connection between m_{weak} and m_{soft} which arises from minimization of the Higgs (scalar) potential of the Minimal Supersymmetric Standard Model (MSSM):

$$m_Z^2/2 = \frac{(m_{H_d}^2 + \Sigma_d^d) - (m_{H_u}^2 + \Sigma_u^u) \tan^2 \beta}{\tan^2 \beta - 1} - \mu^2 \sim -m_{H_u}^2 - \Sigma_u^u(\tilde{t}_{1,2}) - \mu^2 \quad (1)$$

where $m_{H_{u,d}}$ are the Higgs soft SUSY breaking masses, μ is the (SUSY conserving) Higgs mixing term, $\tan \beta = v_u/v_d$ is the ratio of Higgs field vevs and the $\Sigma_{u,d}^{u,d}$ terms contain an assortment of loop corrections (expressions may be found in Ref's [5] and [6]). Under *practical naturalness* [7] – wherein all independent contributions to an observable ought to be comparable to or less than the observable – then only $|m_{H_u}|$ and μ ought to be $\sim m_{weak}$ whilst other particle contributions to the weak scale may be much heavier since their contributions are loop-suppressed. A naturalness measure Δ_{EW} has been proposed [8] which compares the largest contribution to the right-hand-side of Eq. 1 to $m_Z^2/2$. Models with $\Delta_{EW} \lesssim 30$ are then presumed practically natural and for such models there is no LHP.

One consequence of natural SUSY is that of all the sparticles, one expects only the higgsinos (with mass $\sim |\mu|$) to be of order m_{weak} . Higgsino pair production is difficult to observe at LHC due to the small inter-higgsino mass gap [9], and limits on μ vary between $\gtrsim 100 - 200$ GeV depending on the mass gap $\Delta m_{21} = m_{\tilde{\chi}_2^0} - m_{\tilde{\chi}_1^0}$ [10]. A challenge for LHC Run 3 and high-lumi LHC (HL-LHC) is to either discover light higgsinos or else rule out natural SUSY by excluding the higgsino discovery plane [11]. At present, both ATLAS [12] and CMS [13] seem to have $\sim 2\sigma$ excesses in the opposite-sign-dilepton-plus-jet-plus-MET (OSDLJMET) signature [14, 15]; upcoming new data should either confirm or exclude such signal channels.

Unnatural SUSY with large $|\mu| \gg m_{weak}$, while possible, seems at first glance highly implausible. However, model builders have proposed a way to remain natural even with $|\mu| \gg m_{weak}$ by discovering models where the *combinations* $m_{H_{u,d}}^2 + \mu^2$ are driven to be tiny, while $\sqrt{|m_{H_{u,d}}^2|}$ and μ individually can each be large at the weak scale. This method is called *scalar sequestering* (SS) [16–19].

The method of hidden sector sequestering (HSS) of visible sector operators arises from postulating the existence of a strongly interacting nearly superconformal hidden sector (HS) which is operative between the messenger scale M_* (taken to be of order the reduced Planck

mass $\sim m_P$ in the case of gravity mediation) and a much lower intermediate scale M_{int} where the superconformal symmetry is broken and SUSY is also broken. This method of sequestering was originally proposed [20] as a means to obtain anomaly-mediated SUSY breaking (AMSB) models [21, 22] when geometric sequestering was shown to be difficult to realize [23].

Under HSS, the various soft SUSY breaking terms get squeezed to tiny values via RG running between m_* and M_{int} by a power-law behavior:

$$m_{soft}(M_{int}) \sim (M_{int}/m_*)^\Gamma m_{soft}(m_*) \quad (2)$$

where the exponent Γ includes combinations of classical and anomalous dimensions of HS fields S . Γ is not directly calculable due to the strong dynamics in the HS but is instead assumed to be ~ 1 . For $M_{int} \sim 10^{11}$ GeV and $\Gamma \sim 1$, then the suppression of gravity-mediated soft terms can be $\sim 10^{-7}$ in which case the AMSB soft terms would be dominant. Additional symmetries seemed to be required in order for HSS to be viable; nonetheless, the lesson was that (model dependent) hidden sector effects could potentially modify the assumed running of SUSY model parameters as expected under the MSSM only [24, 25]. HSS was then found to offer a solution to the needed suppression of various problematic operators. For instance, in gauge mediation [26] the $B\mu$ soft term is expected with $B\mu \gg \mu^2$, leading to the famous $B\mu/\mu$ problem. HSS could be used to suppress $B\mu(M_{int}) \sim 0$ thus solving the problem [16, 27]. Also, in gravity mediation, scalar masses arise via hidden sector-visible sector couplings such as

$$\int d^4\theta \frac{c_{ij}}{m_P^2} S^\dagger S Q_i^\dagger Q_j \quad (3)$$

where the Q_i are visible sector fields and the S are hidden sector fields which acquire an auxiliary field SUSY breaking vev $F_S \sim (10^{11} \text{ GeV})^2$. In gravity-mediation, such operators are unsuppressed by any known symmetry (leading to the SUSY flavor problem), but could be squeezed to tiny values via scalar sequestering. A third application of (scalar) sequestering is to ameliorate the LHP while maintaining large μ values: $|\mu| \gg m_{weak}$. This case, which is the subject of the present paper, makes use of Eq. 3 to suppress via hidden sector running all scalar masses to ~ 0 . However, in the case where the Giudice-Masiero (GM) mechanism [28] is assumed¹ to generate a weak scale value of μ , then the scalar sequestering actually applies to m_Q^2 for matter scalars, but to the combinations $m_{H_{u,d}}^2 + \mu^2$ for Higgs scalars. In this case, at the intermediate scale M_{int} , then one expects $m_Q^2 \sim 0$ but with $m_{H_{u,d}}^2 \sim -\mu^2$ so that μ can be large whilst the combination $m_{H_{u,d}}^2 + \mu^2$ is small: this has the potential to fulfill the naturalness requirement in Eq. 1 while maintaining large $|\mu| \gg m_{weak}$ since μ^2 and $m_{H_{u,d}}^2$ are no longer independent.

In this paper, we examine the phenomenology of SUSY models with scalar sequestering. In Sec. 2, we present a brief review of the theory underlying scalar sequestering. Two different theory approaches have emerged: strong scalar sequestering where hidden sector running overwhelms MSSM running [16, 17], and moderate scalar sequestering [19], wherein hidden sector running and MSSM running are comparable, leading to quasi-fixed point behavior for the intermediate scale soft term boundary conditions. In Sec. 3, we examine strong SS, dubbed here

¹Twenty solutions to the SUSY μ problem are reviewed in Ref. [29]

as the PRS (Perez, Roy and Schmaltz) scheme [17]. Here, the intermediate scale boundary conditions are so determinative that only one (or a few) parameters completely determine the SUSY phenomenology. In this case, problems emerge for appropriate electroweak symmetry breaking, vacuum stability, and dark matter physics (with typically a charged LSP and sometimes a left-sneutrino LSP). The latter case with a charged LSP can be dispensed with via either an assumed R -parity violation [30, 31] or assumed LSP decays to non-MSSM DM particles such as an axino \tilde{a} [32]. In Sec. 4, we verify these results with parameter space scans in the PRS scheme with and without unified gaugino masses. In Sec. 5, we instead adopt the scheme in [19] – we refer to this scheme as SPM (Stephen P. Martin)– with more limited HS running which is comparable to MSSM running. In this scheme, for the case of unified gaugino masses (UGM), we find that although SS reduces the amount of EW finetuning, significant weak scale finetuning arising from large top-squark masses remains, so that the finetuning problem cannot be said to be eliminated for large μ . However, in the case of non-universal gaugino masses (NUGM) which lead to large stop mixing and $m_h \simeq 125$ GeV, then evidently low finetuning along with appropriate EWSB can be achieved for more moderate values of $\mu \sim 1$ TeV. Our findings are summarized in Sec. 6.

2 Brief review of scalar sequestering

Let us assume a gravity-mediated generation of soft SUSY breaking terms since gauge-mediation gives rise to trilinear soft terms $A \sim 0$ and hence requires large, unnatural values of top squarks [33] to generate $m_h \sim 125$ GeV [34]. At some scale $m_* < m_P$, the (superconformal) hidden sector becomes strongly interacting. Its coupling to visible sector fields leads to suppression of scalar soft breaking masses and also the bilinear soft term $b \equiv B\mu$. At some intermediate scale M_{int} , the conformal symmetry is broken and the hidden sector is integrated out of the low energy EFT. Also around this scale, SUSY is broken at a scale $Q_{SUSY}^2 \sim F_S$.

Under gravity-mediation, the following operators give rise to the usual soft terms:

$$\int d^2\theta c_\lambda \frac{S}{m_P} WW + h.c. \Rightarrow m_\lambda \sim c_\lambda (F_S/m_P), \quad (4)$$

$$\int d^2\theta c_A \frac{S}{m_P} \phi_i \phi_j \phi_k + h.c. \Rightarrow A_{ijk} \sim c_A (F_S/m_P), \quad (5)$$

$$\int d^4\theta c_{ij} \frac{R}{m_P^2} \phi_i^\dagger \phi_j \Rightarrow m_{\phi_{ij}}^2 \sim c_{ij} (F_S/m_P)^2, \quad (6)$$

and

$$\int d^4\theta c_b \frac{R}{m_P^2} H_u H_d + h.c. \Rightarrow B\mu \sim c_b (F_S/m_P)^2, \quad (7)$$

where S is a HS chiral superfield and R is a real product of hidden sector fields with $R \sim S^\dagger S + \dots$. In addition, for the scalar sequestering model, one assumes the μ term is initially suppressed (by some symmetry?) but then arises via the Giudice-Masiero [28] mechanism at the scale m_{soft} via

$$\int d^4\theta c_\mu \frac{S^\dagger}{m_P} H_u H_d \Rightarrow \mu_{GM} \sim c_\mu (F_S/m_P). \quad (8)$$

The holomorphic terms ($\int d^2\theta$) are protected against renormalization effects by non-renormalization theorems but the non-holomorphic terms are not. The latter terms give rise to scalar masses $m_{\phi_{ij}}^2$ and the bilinear soft term $B\mu$, and will scale between m_* and M_{int} as $(M_{int}/m_*)^\Gamma$ where the exponent Γ is related to the anomalous dimension of the S field.

While Γ is not directly calculable since the HS is strongly interacting, under the assumption that Γ is large and positive, *e.g.* ~ 1 , then the factor $(M_{int}/m_*)^\Gamma$ can lead to large suppression of scalar masses and $B\mu$ as compared to gaugino masses, A -terms and μ . However, while μ can remain large under scalar sequestering, the combination $\hat{m}_{H_{u,d}}^2 \equiv m_{H_{u,d}}^2 + \mu^2$ gets driven to tiny values by the $(M_{int}/m_*)^\Gamma$ factor.

3 Scalar sequestered SUSY: PRS boundary conditions

In the PRS scheme [16,17], the SS is assumed to dominate any MSSM running of soft terms. In this case, one expects the usual MSSM running for gaugino masses, A -terms and μ between the high scale m_* and the intermediate scale M_{int} , whilst HS effects suppress matter scalar masses $m_{\phi_{ij}}^2$, $B\mu$ and Higgs combinations $m_{H_{u,d}}^2 + \mu^2$. Thus, (under the assumption of unified gaugino masses) the parameter space of the model is given by

$$m_{1/2}, A_0, \mu \quad \text{and} \quad M_{int} \quad (9)$$

where the first three of these are given at the high scale m_* . Motivated by gauge coupling unification, we take $m_* = m_{GUT}$, the scale where g_1 and g_2 unify under MSSM running, and where $m_{GUT} \simeq 2 \times 10^{16}$ GeV. Meanwhile, the matter scalar masses, $B\mu$ and $m_{H_{u,d}}^2 + \mu^2$ are taken to be ~ 0 at the scale $Q \sim M_{int}$.

3.1 Results for $M_{int} = 10^{11}$ GeV and $A_0 < 0$

As an illustration, we show in Fig. 1 the running of soft terms and μ for the case where $m_{1/2} = -A_0 = 1.5$ TeV with $\mu = 500$ GeV (the reason for $\mu \sim 500$ GeV is to be explained shortly). The pink shaded region shows the superconformal regime, whilst the soft terms run according to MSSM-only RGEs in the left-side unshaded region. We see from frame *a*) that the matter scalars start running at $Q = 10^{11}$ GeV where the squark masses are pulled to large values $\gtrsim 2$ TeV due to the influence of the $SU(3)$ gaugino mass M_3 . Left-slepton masses are pulled up by a large $SU(2)_L$ gaugino mass M_2 to the vicinity of ~ 650 GeV at m_{weak} whilst the right slepton masses are pulled up by the $U(1)_Y$ gaugino mass M_1 to ~ 300 GeV. The running of the bilinear b -term is given at the one-loop level by

$$\frac{db}{dt} = \frac{\beta_b^{(1)}}{16\pi^2} \quad (10)$$

where the one-loop beta function is given by

$$\beta_b^{(1)} = b(3f_t^2 + 3f_b^2 + f_\tau^2 - 3g_2^2 - \frac{3}{5}g_1^2) + \mu(6a_t f_t + 6a_b f_b + 2a_\tau f_\tau + 6g_2^2 M_2 + \frac{6}{5}g_1^2 M_1) \quad (11)$$

where the f_i are Yukawa couplings, the g_i are gauge couplings, the $a_i = A_i f_i$ are the reduced trilinear couplings, and the M_i are gaugino masses (further RGEs are given in, *e.g.*, Ref. [1], with their two-loop counterparts in Ref. [35]). In our numerical results presented in this paper, we use the full two-loop running of soft terms and gauge and Yukawa couplings.

The $\sqrt{b} = \sqrt{B\mu}$ term is pulled from zero at $Q = M_{int}$ to ~ 550 GeV at $Q = m_{weak}$ mainly by the second term of Eq. 11. Meanwhile, with $\mu = 500$ GeV, the $\text{sign}(m_{H_{u,d}}^2) * \sqrt{|m_{H_{u,d}}|}$ soft terms begin at -500 GeV and $m_{H_u}^2$ is driven to large negative values at m_{weak} due to the large top-quark Yukawa coupling f_t . Also, m_{H_d} is driven dominantly by the gaugino mass M_2 to small negative values ~ -100 GeV at m_{weak} . Frame *b*) shows the running of trilinear soft terms starting from $Q = m_{GUT}$. These terms are pushed to large negative values by the respective gauge interactions. In the case of A_t , this may help drive stop masses towards tachyonic values and consequently to charge and/or color breaking (CCB) minima in the scalar potential.

A major check on this very constrained PRS scheme is if the EW symmetry is properly broken. Let us recall the (tree-level) conditions for proper EWSB. First, one must check whether the scalar potential indeed *does not develop a minimum* at $h_u^0 = h_d^0 = 0$, the origin of neutral scalar field space. The stability of the critical point satisfying

$$\left. \frac{\partial V}{\partial h_u^0} \right|_{h_u^0=h_d^0=0} = \left. \frac{\partial V}{\partial h_d^0} \right|_{h_u^0=h_d^0=0} = 0$$

are determined by the nature of the eigenvalues of the matrix of second derivatives of the scalar potential, V , evaluated at the origin of field space. We refer to this matrix of second derivatives as the Hessian. Here, the neutral scalar fields are denoted $h_{u,d}^0$.

The goal is to have a vacuum whose origin of field space is destabilized, else EWSB fails to occur properly. There are two cases in which this can happen:

1. the origin is a maximum in field space, or perhaps
2. the origin is a saddle point.

To determine the stability of the critical points we find, the type of critical point can be identified using the multivariate second partial derivative test. Case 1 occurs when the determinant of this Hessian is positive, but $m_{H_u}^2 + \mu^2 < 0$ at the SUSY scale; then, the origin of field space will be a maximum. This secondary condition is crucial, meaning the positive determinant *alone* is insufficient here to determine the nature of the critical point at the origin. When the determinant is positive, but $m_{H_u}^2 + \mu^2 > 0$, then the origin of field space will be a *minimum*, hence the scalar fields fail to acquire nonzero VEVs and EWSB fails to occur.

Case 2 occurs when the determinant of the Hessian of the scalar potential at the origin with respect to the neutral Higgs scalars is negative, as this implies its eigenvalues have opposite signs, leading to

$$(B\mu)^2 > (m_{H_u}^2 + \mu^2)(m_{H_d}^2 + \mu^2). \quad (12)$$

This is often referred to in the literature as the condition for having a maximum at the origin of field space, but is more accurately described as a saddle point. In either case of a maximum or a saddle point, the origin is destabilized, so proper EWSB may yet be achievable, barring

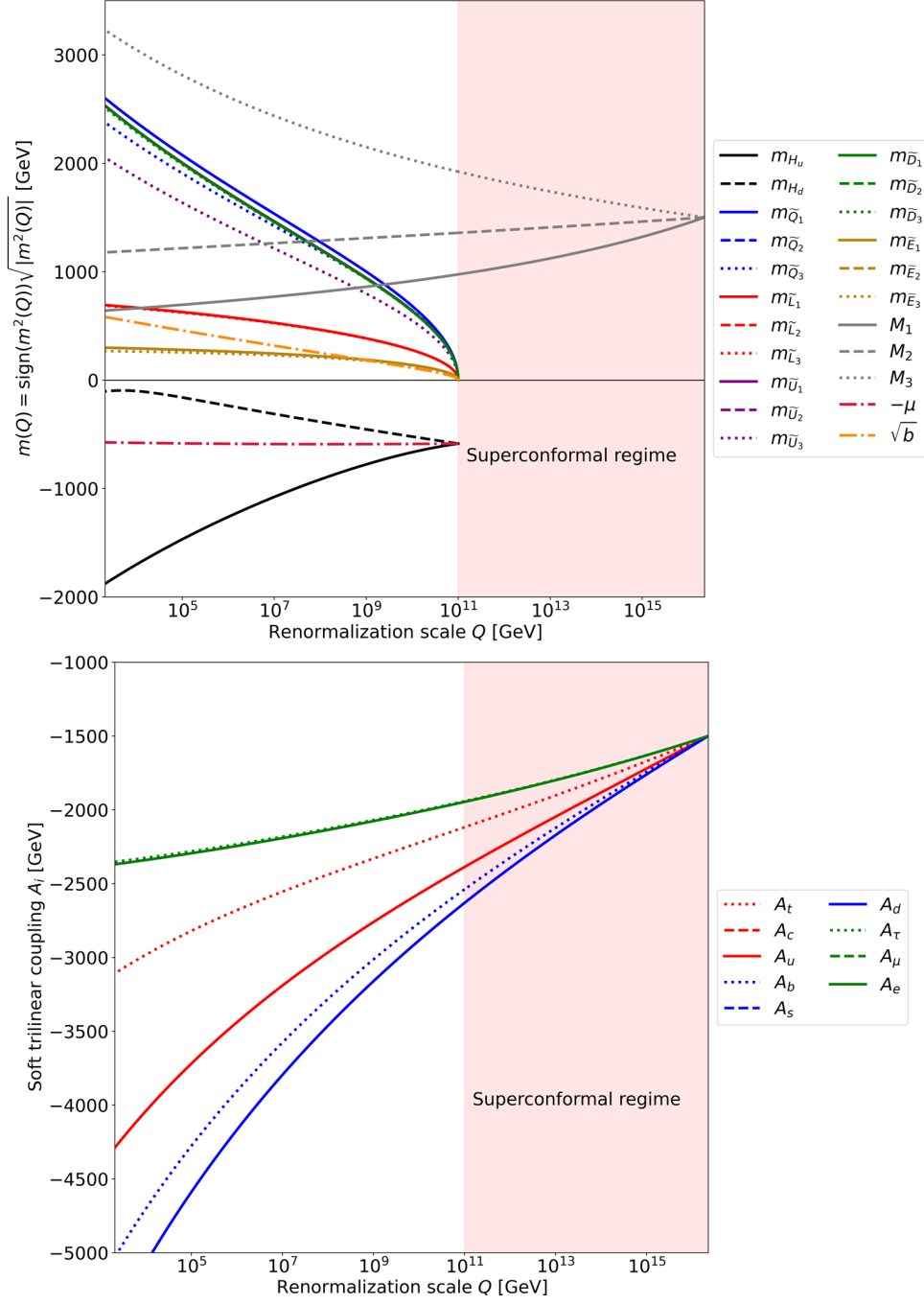


Figure 1: Running of soft terms and $-\mu$ in the PRS scalar sequestering scheme for $m_{1/2} = 1.5$ TeV, $A_0 = -m_{1/2}$, and $\mu = 500$ GeV. We also take the intermediate scale $M_{int} = 10^{11}$ GeV. In frame a) we show running scalar masses and the μ term, while in frame b) we show the running trilinear soft terms.

failure in the conditions below. In particular, given that $m_{H_u}^2$ is driven large negative and $B\mu$ is driven small positive, this saddle point condition may not always occur, but maxima sometimes occur instead as in case 1 and must be checked carefully!

Secondly, one must check that the scalar potential is bounded from below (vacuum stability) in the D -flat direction $h_u^0 = h_d^0$ leading to the requirement that

$$m_{H_u}^2 + m_{H_d}^2 + 2\mu^2 > 2|B\mu|. \quad (13)$$

Given that $m_{H_u}^2$ is large negative, this condition also may be subject to failure, in which case the scalar potential is unbounded from below (UFB).

If an appropriate EWSB occurs, then minimization of the Higgs potential allows one to determine the Higgs vevs v_u and v_d , with $\tan\beta = v_u/v_d$ as usual. The minimization conditions can be recast at tree-level as

$$B\mu = \frac{(m_{H_u}^2 + m_{H_d}^2 + 2\mu^2) \sin(2\beta)}{2} \quad (14)$$

and

$$m_Z^2/2 = \frac{m_{H_d}^2 - m_{H_u}^2 \tan^2\beta}{\tan^2\beta - 1} - \mu^2. \quad (15)$$

Usually, in models like mSUGRA, the first of these is used to trade $B\mu$ for $\tan\beta$ and the second is used to determine the magnitude of μ . In the present case, since the boundary condition for $B\mu$ is ~ 0 at $Q = M_{int}$, it is not available to determine a unique value of $\tan\beta$, since the running of the soft parameters depends on the Yukawa couplings which in turn depend on v_u and v_d , whose values then define $\tan\beta$. Furthermore, from Eq. 15 we see that μ is not freely available to be determined by the measured value of $m_Z = 91.2$ GeV. Thus, the equations 14 and 15 must be used to map out the derived values of m_Z in the μ vs. $\tan\beta$ plane.

This is shown in Fig. 2 for the case at hand. Here, we see that for large μ values, then m_Z^2 is computed at loop level to be negative. For smaller μ , then typically m_Z is of order the TeV scale. For a given value of $\tan\beta$, one can choose μ near the edge of the gray excluded region where $m_Z \sim 100$ GeV. For Fig. 1, we have chosen $\tan\beta = 10$ which then fixes $\mu \sim 500$ GeV. Unfortunately, for all choices of μ and $\tan\beta$ shown in the plane, we find the scalar potential to be UFB in the D -flat direction.

3.2 Results for $A_0 > 0$

In Fig. 3, we show a PRS point that does develop appropriate EWSB where $M_{int} = 4 \times 10^{11}$ GeV and $m_{1/2} = A_0 = 1$ TeV. For $\tan\beta = 21.25$, we find $\mu \simeq 1.8$ TeV. In this case, with $A_0 = 1$ TeV, we see from frame *b*) that the A_i parameters are all positive for large Q , with A_t and A_b becoming small and then negative around $Q \lesssim 10^{10}$ GeV. This feeds into the b parameter evolution causing b to run at $Q < M_{int}$ to negative values until the large negative A_i terms cause it to turn up and become positive around $Q \sim m_{weak}$, aiding in appropriate EWSB. While this model does develop a viable EW vacuum, the slepton masses evolve only to $m_{E_i} \sim 250$ GeV at $Q \sim m_{weak}$ so that slepton masses are well below both the μ and M_1 terms. Thus, for this point we have a charged slepton as the lightest SUSY particle. The derived sparticle mass spectra for this case are shown in Fig. 4.

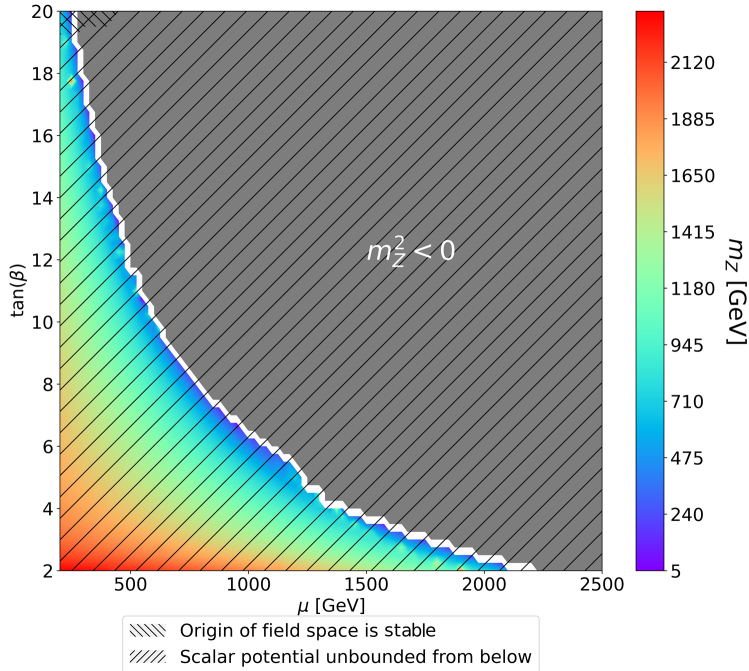


Figure 2: Computed value of m_Z in the μ_{GUT} vs. $\tan\beta$ plane for the PRS BM point with $m_{1/2} = -A_0 = 1.5$ TeV, and $M_{int} = 10^{11}$ GeV.

In the case shown, with the MSSM-only as the low energy EFT, then one would expect a charged stable relic, and dark matter wouldn't be dark. One can circumvent this situation by adding extra particles or interactions to the low energy EFT. An example of the former would be to add a Peccei-Quinn (PQ) sector with an axino \tilde{a} as the LSP so that $\tilde{e}_R \rightarrow e\tilde{a}$. In this case, one would get a potentially long-lived but unstable slepton and one must avoid collider and other constraints on such objects. The slepton lifetime would depend on the assumed value of the PQ scale f_a . An example of added interactions would be to postulate broken R -parity so that the slepton LSP decays to SM particles. Then one must explain why some RPV couplings are substantial whilst others are very small, as required by proton stability bounds [30, 31].

4 Parameter space scans: PRS scheme

4.1 Universal gaugino masses

In order to search for viable weak scale SUSY spectra in the PRS scheme, we implement a scan over the PRS parameter space:

- $m_{1/2} : 0.2 \rightarrow 5$ TeV
- $A_0 : -5 \rightarrow +5$ TeV
- $M_{int} : 10^6 \rightarrow 10^{14}$ GeV.

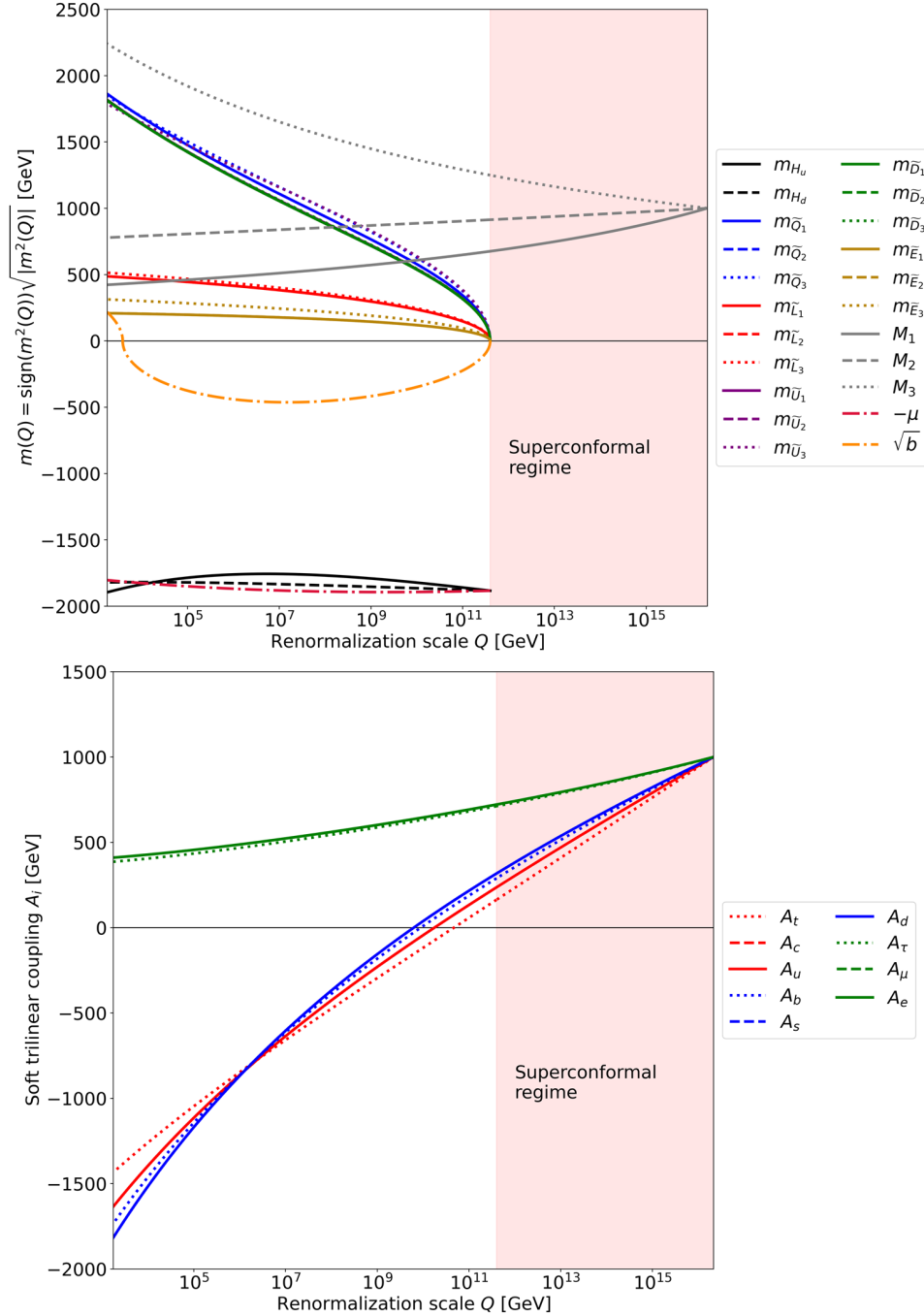


Figure 3: Running of soft terms and μ in the PRS scalar sequestering scheme for $m_{1/2} = 1$ TeV, $A_0 = m_{1/2}$, and $\mu = 1.8$ TeV. We take the intermediate scale $M_{int} = 4 \times 10^{11}$ GeV. In frame *a*) we show running scalar masses and μ term while in frame *b*) we show the running trilinear soft terms.

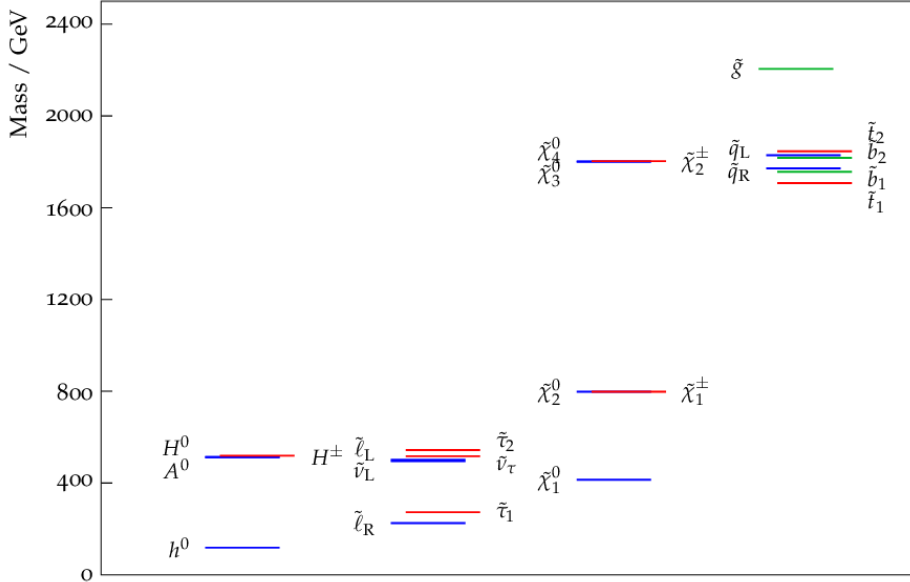


Figure 4: The resulting mass spectrum with a characteristic slepton as the LSP for the PRS scheme with $m_{1/2} = 1$ TeV, $A_0 = m_{1/2}$, and $\mu = 1.8$ TeV. The spectrum was produced using SoftSUSY v4.1.17 [36] and slhaplot [37].

Our code then scans over values of $(\mu, \tan \beta)$ leading to $m_Z \sim 91.2$ GeV. We then check for CCB minima, points that are UFB, and appropriate EWSB. For points that pass all criteria with appropriate EWSB, we then check for a neutral or a charged LSP.

Our first results are shown in Fig. 5 where we show scan points *a*) in the A_0 vs. M_{int} plane and *b*) in the A_0 vs. $m_{1/2}$ plane. From frame *a*), we see that only the yellow points satisfy all EWSB constraints, although all the surviving points have a slepton as the LSP. In particular, the $A_0 < 0$ points almost all have either CCB minima (for large negative A_0) or else an UFB potential. For $A_0 > 0$, then the scalar potential is better behaved but frequently does not have appropriate EWSB. The scan points with appropriate EWSB are much more prominent at large M_{int} and large $m_{1/2}$.

In Fig. 6, we show our scan points in the $m_{1/2}$ vs. μ plane. Here, we see some structure where $\mu \sim 2m_{1/2}$ is favored. These qualitative features were also found by Perez, *et al.* in Ref. [17] where most of their parameter space was excluded by EWSB constraints except for large M_{int} where they also found $\mu \sim 2m_{1/2}$ and for their lone sample point, they also obtained a slepton as the LSP.

Given our overall scan results in the PRS scheme, we find the strong scalar sequestering scenario (with unified gaugino masses) rather difficult (but not impossible) to accept: the bulk of p-space points have problematic EWSB and any surviving points have a charged LSP thus requiring new particles and/or new interactions to evade cosmological constraints on charged relics from the Big Bang.

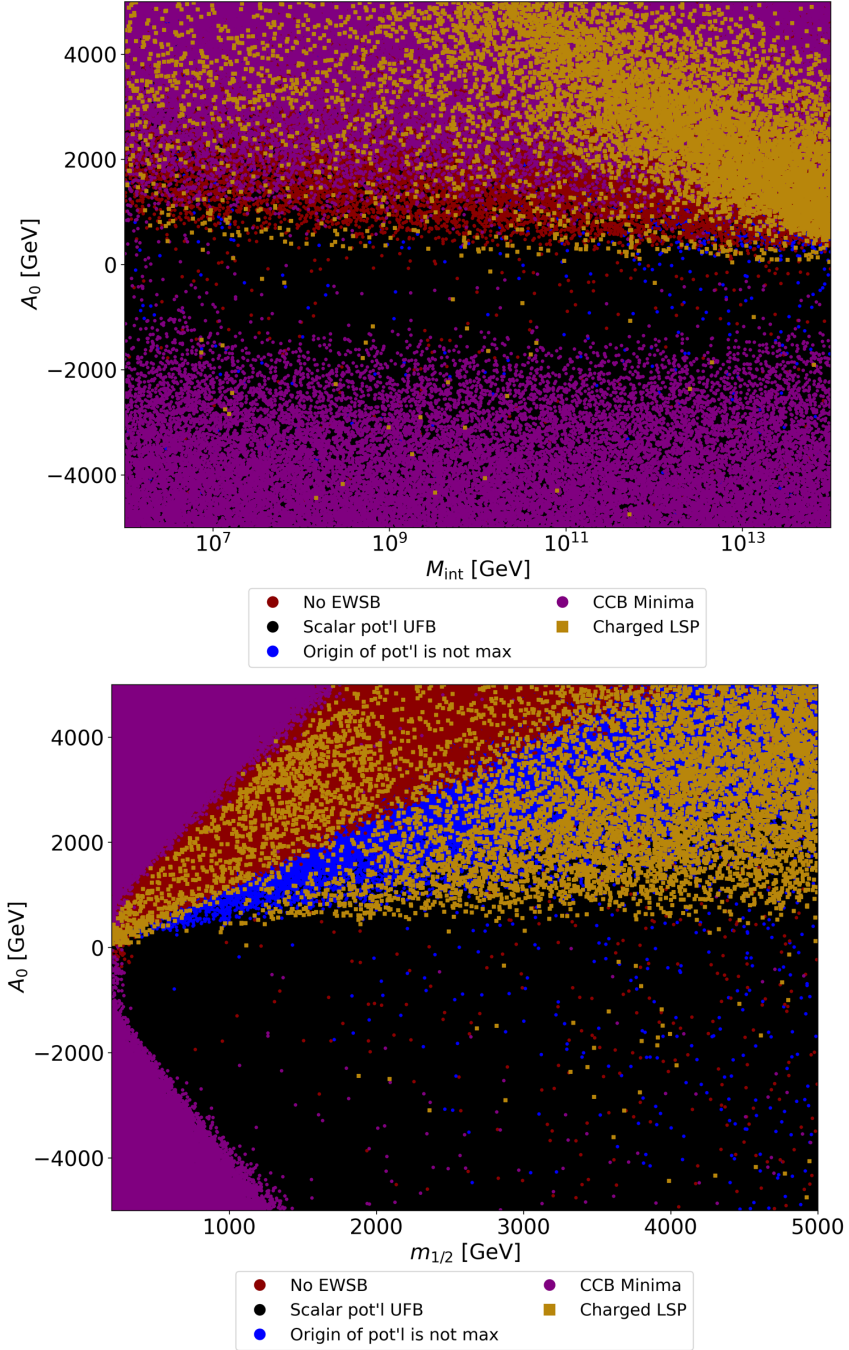


Figure 5: Scan over the PRS parameter space with UGMs in the a) A_0 vs. M_{int} plane and b) the A_0 vs. $m_{1/2}$ plane.

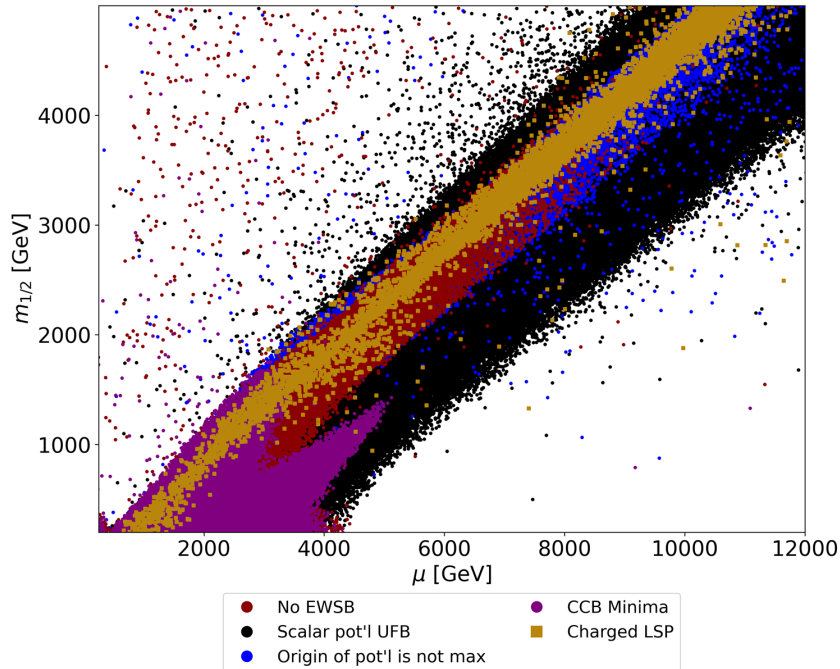


Figure 6: Scan over the PRS parameter space with UGMs in the $m_{1/2}$ vs. μ plane.

4.2 Non-universal gaugino masses

4.2.1 Varying M_1 and M_2

One possibility to try to circumvent the slepton-LSP problem in the PRS scheme is to appeal to NUGMs, by dialing down either M_1 or M_2 from their unified values until either the bino or the wino becomes the LSP. The computed sparticle mass spectra are shown in Fig. 7 in frame *a*) for varying M_1 and in frame *b*) for varying M_2 . From frame *a*), we see that as M_1 diminishes, the lightest neutralino mass $m_{\tilde{\chi}_1^0}$ does indeed decrease (moving from unified gaugino masses on the right to small M_1 on the left as shown by the lavender dashed curve). However, as M_1 decreases, then upward RGE pull on m_{E_i} (right-slepton soft mass of generation i) from the $U(1)_Y$ gaugino also diminishes, and ultimately $m_{E_{1,2}}^2$ go tachyonic around $M_1 \sim 0.23m_{1/2}$. Note in this case that the stau soft mass remains larger due to a large negative X_τ term in the $m_{E_3}^2$ RGE owing to large negative $m_{H_d}^2$. This is shown in Fig. 8 which shows the soft mass running for a case with small M_1 compared to $m_{1/2}$. This behavior where the bino fails to become LSP in the PRS scheme with small M_1 appears rather general when we scan over all M_1 values (to be shown shortly).

Likewise, in frame *b*), we take M_2 to be its unified value on the right-side of the plot, and then dial its value down to try to gain a wino as LSP. Around $M_2 \sim 0.58m_{1/2}$, the $m_{\tilde{\chi}_1^\pm}$ and $m_{\tilde{\chi}_1^0}$ mass curves coincide, showing that the lightest neutralino has gone from bino to wino. However, in this case, the right-sleptons remain LSP until $M_2 \sim 0.35m_{1/2}$ whence the left sleptons, and particularly here the left-sneutrino, becomes LSP. Left-sneutrinos have direct detection cross sections for scattering on Xe nuclei of $\sigma(\tilde{\nu}_{eL}Xe \rightarrow \tilde{\nu}_{eL}Xe)$ of $\sim 4.5 \times 10^{-23} \text{ cm}^2$ [38], about

23 orders of magnitude large than current LZ limits [39], and so are excluded as dark matter. For somewhat lower values of M_2 , then $B\mu$ runs to very small values, leading to a UFB scalar potential. This behavior also seems rather general from our PRS scan with NUGMs.

4.2.2 Scan over PRS scheme with NUGMs

For completeness in our search for viable weak scale SUSY spectra in the PRS scheme, we can adopt the case of non-universal gaugino masses and scan over this expanded parameter space:

- $M_1(\text{GUT}) : 0.2 \rightarrow 5 \text{ TeV}$
- $M_2(\text{GUT}) : 0.2 \rightarrow 5 \text{ TeV}$
- $M_3(\text{GUT}) : 0.2 \rightarrow 5 \text{ TeV}$
- $A_0 : -5 \rightarrow +5 \text{ TeV}$
- $M_{int} : 10^6 \rightarrow 10^{14} \text{ GeV}$.

Similar to above, our code then finds pairs of $(\mu, \tan\beta)$ leading to $m_Z \sim 91.2 \text{ GeV}$. We then check for CCB minima, points that are UFB, and appropriate EWSB. For points that pass all criteria with appropriate EWSB, we then check for a neutral or a charged LSP along with LHC constraints on the gluino mass and lightest stop mass. As discussed above, one may try to dial down the $M_1(\text{GUT})$ parameter to obtain a neutralino LSP, though this leads to both CCB and EWSB issues in this model. The issue of a charged LSP persists as in the UGM case, though it is possible to accommodate a sneutrino LSP in some cases, when $M_2(\text{GUT}) < M_1(\text{GUT})$. However, this scenario is severely ruled out due to direct dark matter detection constraints.

Our non-universal gaugino mass scan results are demonstrated in Fig. 9 where we show scan points *a*) in the A_0 vs. M_{int} plane and *b*) in the $M_1(\text{GUT})/M_2(\text{GUT})$ vs. $M_3(\text{GUT})$ plane. Even with NUGMs, we do not find any points where EWSB is appropriately broken but without a charged slepton or left-sneutrino LSP.

5 Scalar sequestered SUSY: SPM approach

In the SPM approach [19], it is noticed that there exist bounds on the scaling dimension Γ such that Γ is positive but not too large, with $\Gamma \sim 0.3$ maximally [40–42]. In this case, the superconformal running may be much less, and comparable to the MSSM running. Let us denote the dimension 1 soft breaking terms as m_1 and dimension 2 soft terms as m_2 . Then, after several field rescalings, the dimension-1 terms (the M_i , a_{ijk} and μ) run according to

$$\frac{dm_1}{dt} = \beta_{m_1}^{MSSM} \quad (16)$$

while dimension-2 terms (matter scalars $m_{\phi_{ij}}^2$, $\hat{m}_{H_{U,d}}$ and b) run as

$$\frac{dm_2}{dt} = \Gamma m_2^2 + \beta_{m_2}^{MSSM} \quad (17)$$

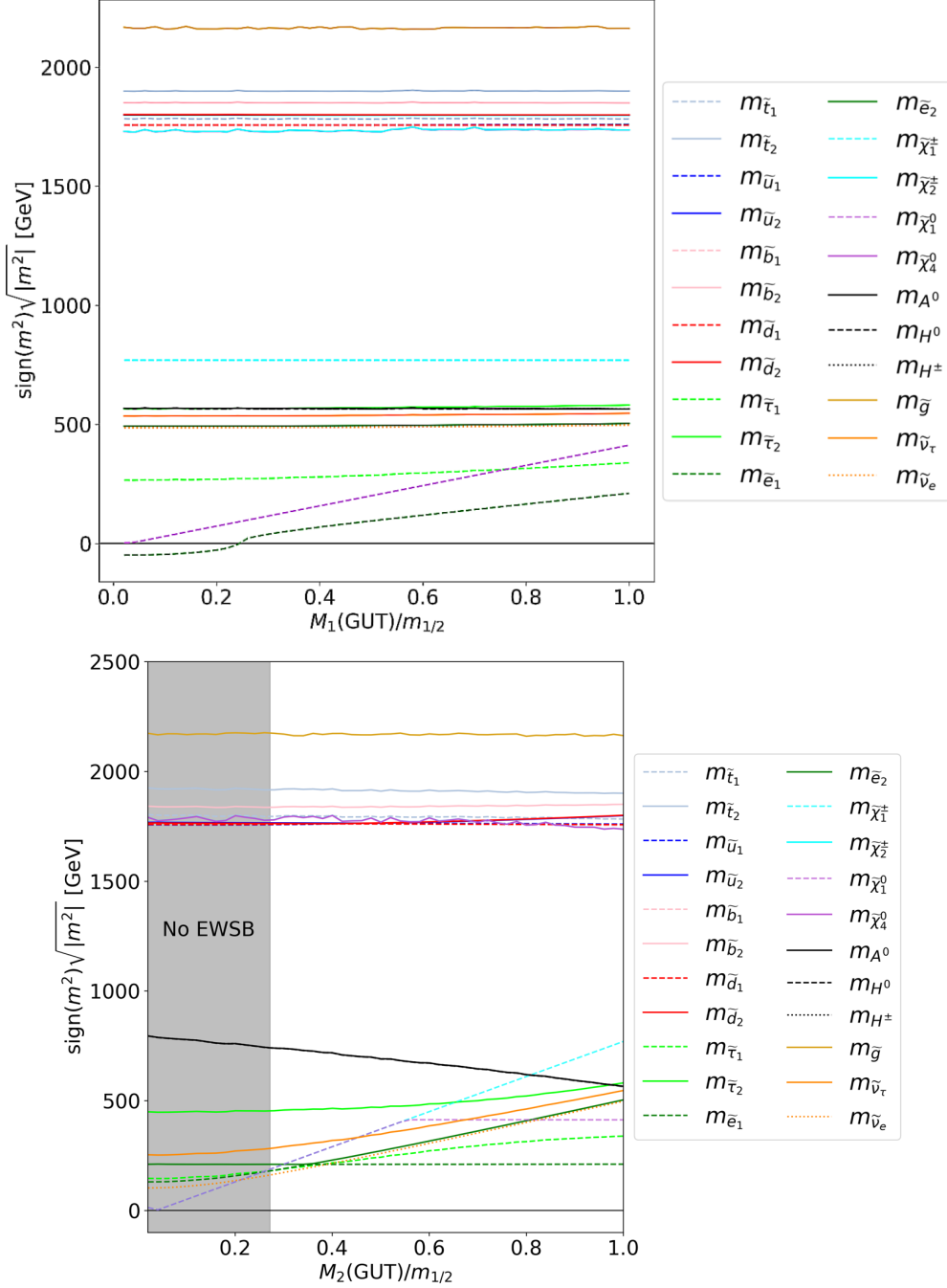


Figure 7: The SUSY mass spectrum vs. GUT-scale gaugino mass parameters M_1, M_2 in the PRS model varied below $m_{1/2}$. In both frames, the spectrum at the far right is similar to the spectrum seen in Fig. 4. In frame a) the mass spectrum as $M_1(\text{GUT})$ is varied below $m_{1/2}$ to zero is plotted. The neutralino never becomes the LSP, as the selectron and smuon remain lighter until CCB minima are realized. In frame b) we display the mass spectrum as $M_2(\text{GUT})$ is varied below $m_{1/2}$ to zero. Near $M_2 \sim 0.4m_{1/2}$, the sneutrino briefly becomes the LSP before the Higgs potential becomes unbounded from below due to a lack of running in the $b = B\mu$ parameter. Thus, a neutralino LSP cannot be achieved here. In both frames, we take $m_{1/2} = M_3(\text{GUT}) = A_0 = 1$ TeV, $M_{\text{int}} = 4 \cdot 10^{11}$ GeV, and $\tan(\beta) = 21.25$.

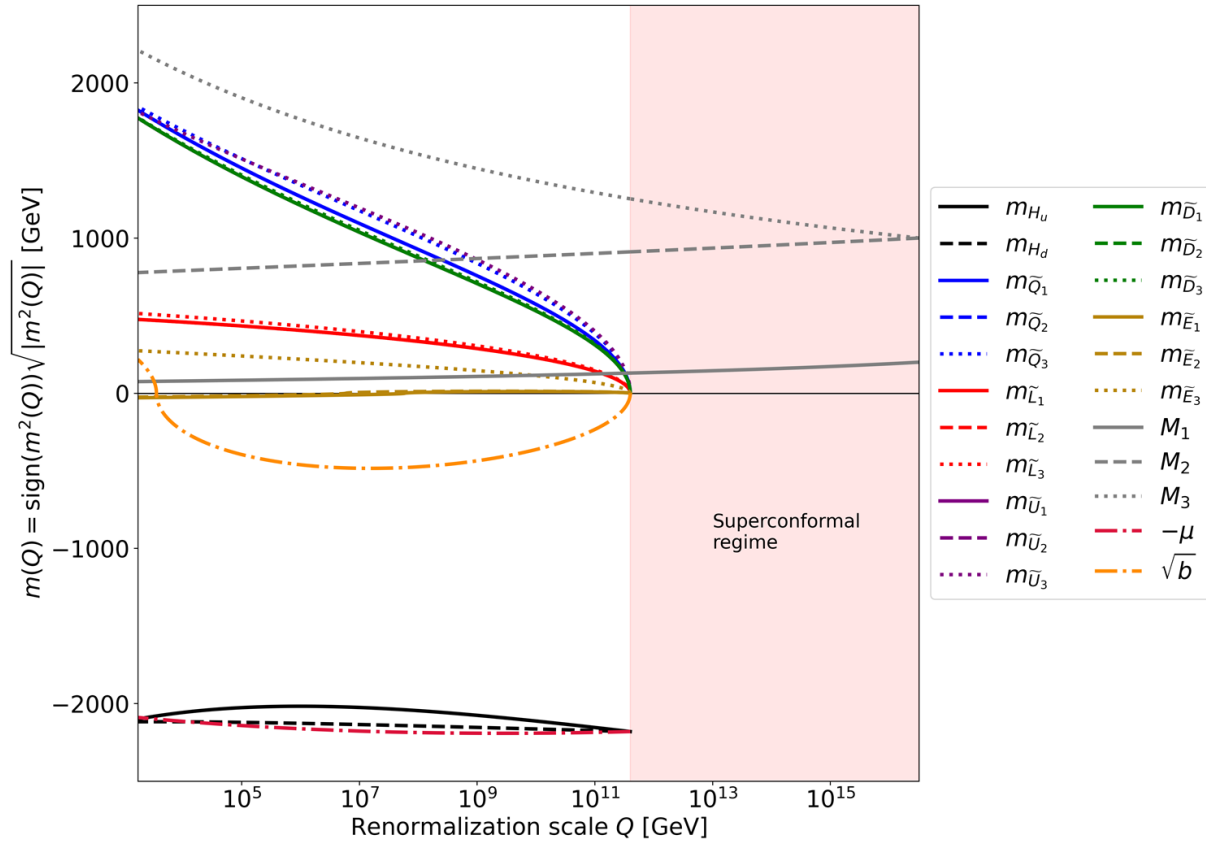


Figure 8: Example RGE running of the soft masses from Fig. 7a) demonstrating the CCB nature of a point with $m_{\tilde{e}_R}^2 < 0$ with $M_1(\text{GUT}) \sim 0.15m_{1/2}$. Though the left-handed slepton states (red) evolve to moderate values, the right-handed slepton states of the first two generations evolve to be negative at the SUSY scale due to the small value of M_1 .

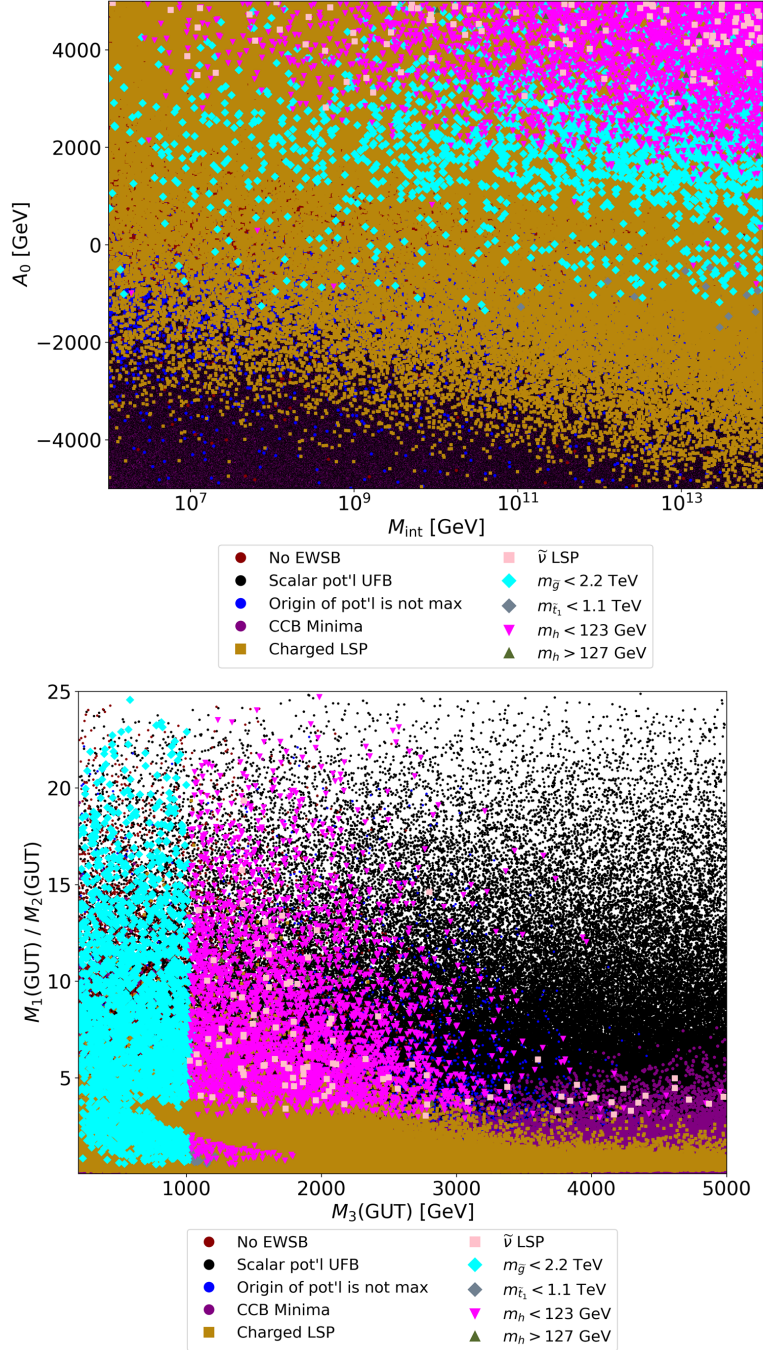


Figure 9: Scan over the PRS parameter space with NUGMs in the a) A_0 vs. M_{int} plane and b) the $M_1(\text{GUT})/M_2(\text{GUT})$ vs. $M_3(\text{GUT})$ plane.

where the β^{MSSM} are the usual MSSM beta functions and $t = \log(Q/Q_0)$ where Q is the energy scale and Q_0 is a reference scale. For the superconformal regime with $M_{int} < Q < m_*$, then $\Gamma \neq 0$ but for $Q < M_{int}$, then the superconformal symmetry is broken and integrated out, and $\Gamma \rightarrow 0$.

An intriguing effect in this case is that the m_2^2 terms can run until $\Gamma m_2^2 \simeq \beta_{m_2}^{MSSM}$ which defines a *quasifixed point* for the m_2^2 running at $m_2^2 \simeq -\beta_{m_2}^{MSSM}/\Gamma$. Approximate expressions for the fixed point values are given by SPM [19], but will not be repeated here. Thus, the m_2^2 terms tend to approach their quasifixed point values as $Q \rightarrow M_{int}$ instead of zero, as in the PRS scheme. This behavior helps to ameliorate the problems of the PRS scheme with respect to EWSB.

The approach to the quasifixed point values are shown in Figs. 10 and 11 for several m_2^2 cases (some of these results verify similar plots by SPM but are presented again here for the benefit of the reader [19]). In Fig. 10, we show running of *a)* the bilinear soft term $B \equiv b/\mu$, *b)* running of $m_{\tilde{u}_R}$ and M_3 and *c)* running of $m_{\tilde{e}_R}$ and M_1 . In all frames, we take $m_{1/2} = 4.5$ TeV, $M_{int} = 10^{11}$ GeV with all matter and Higgs soft masses (and bilinear b) set to m_0 (m_0^2). A different curve is plotted for different values of m_0 ranging from 1 GeV to 10 TeV. The values of A_0 and μ are solved for in each individual curve. Blue curves are for $\mu > 0$ while purple curves are for $\mu < 0$. From frame *a)*, we see the quasi-fixed point for b/μ is largely small but negative. From frame *b)*, we see that the typical squark mass approaches (in this case) a quasi-fixed point value around ~ 2 TeV rather than zero as in the PRS scheme; this helps avoid CCB minima in the SPM scheme. Squark soft masses are then pulled to large values at m_{weak} due to the large value of M_3 which is chosen. From frame *c)*, we see that typical slepton masses approach ~ 1 TeV at M_{int} in SPM rather than zero as in PRS. This helps avoid slepton LSP issues in the SPM scheme.

In Fig. 11, we show in frame *a)* the running of $sign(\hat{m}_{H_u}^2)\sqrt{|\hat{m}_{H_u}^2|}$. This also runs to a quasi-fixed point, in this case around ~ 2 TeV. In frame *b)*, we show the individual running of $m_{H_u}^2$ and μ . While μ runs nearly flat as expected, $m_{H_u}^2$ runs at first to large negative values, and then below M_{int} runs nearly flat. This example may assuage concerns that the running of $m_{H_u}^2$ below M_{int} may destroy its correlation with μ so that the two terms regain some measure of independence: this doesn't seem to happen. In frame *c)*, the running of $\hat{m}_{H_d}^2$ is shown and again it runs to a quasi-fixed point around 2 TeV.

In the SPM scheme, the m_2^2 values approach (but do not exactly meet) their quasifixed point values at $Q = M_{int}$, so that the boundary conditions at $Q = M_{int}$ are no longer fixed. Thus, to generate a workable model, we must expand the parameter space from the PRS scheme. For SPM, therefore, one must reintroduce the various m_2^2 boundary conditions at $Q = m_*$, and we will take

$$m_0, m_{1/2}, A_0, \mu, b = B\mu. \quad (18)$$

After checking for appropriate EWSB, and then employing the EWSB minimization conditions, one can again solve for the derived value of m_Z . This is shown in Fig. 12 where we show color-coded regions of m_Z in the A_0 vs. $\mu(GUT)$ plane for $m_0 = 10$ TeV, $m_{1/2} = 4.5$ TeV and $\tan\beta = 15$. From the plot, one sees that there is no unique solution for $m_Z \simeq 91.2$ GeV but rather two disconnected regions depending on the sign of μ , with a different μ value being obtained for each choice of A_0 .

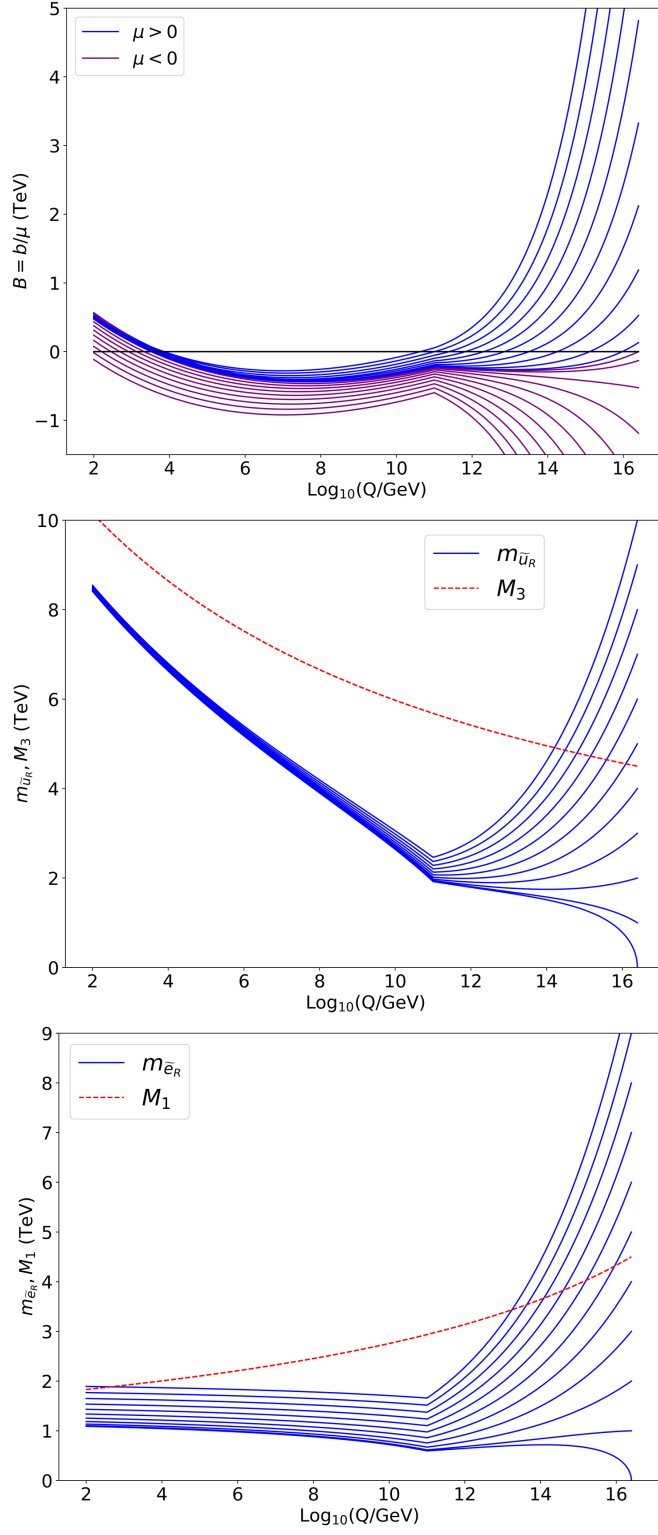


Figure 10: Running of a) $B \equiv b/\mu$, b) m_{U_1} and M_3 and c) m_{E_1} and M_1 from $Q = m_{GUT}$ to $Q = m_{weak}$ under the SPM scheme with $\Gamma = 0.3$.

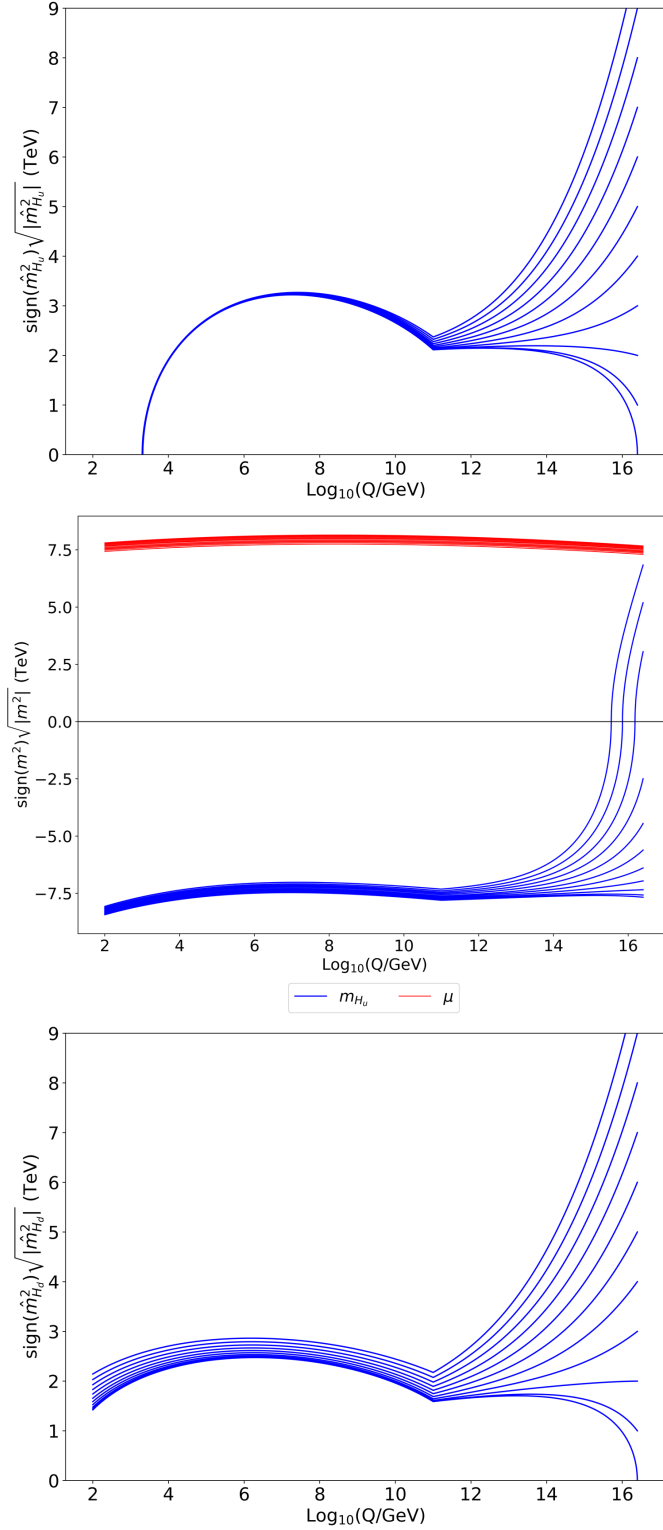


Figure 11: Running of a) $\hat{m}_{H_u}^2$, b) $m_{H_u}^2$ and μ and c) $\hat{m}_{H_d}^2$ from $Q = m_{GUT}$ to $Q = m_{weak}$ under the SPM scheme with $\Gamma = 0.3$.

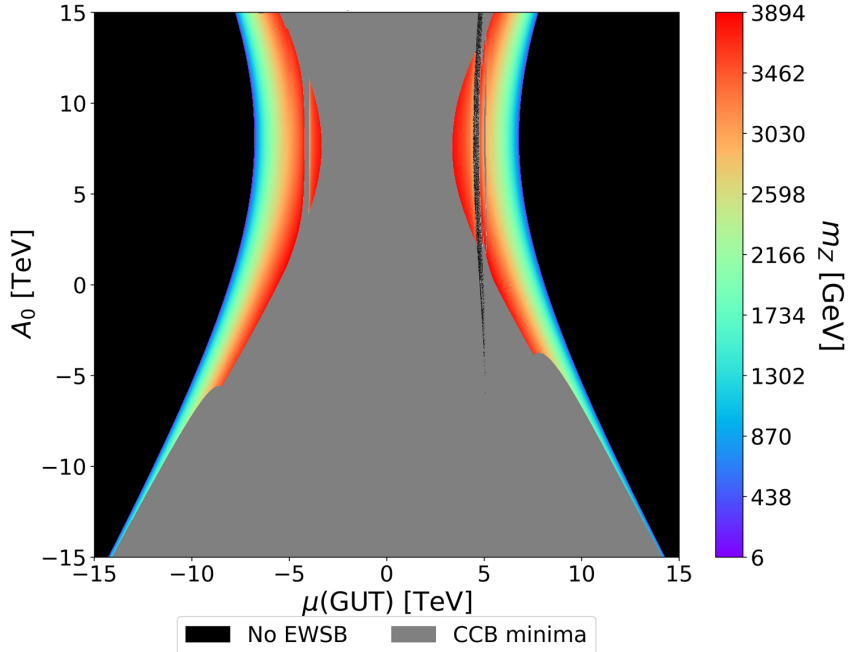


Figure 12: Color-coded regions of the derived value of m_Z in the μ vs. A_0 plane for $\tan\beta = 15$ with $m_0 = 10$ TeV and $m_{1/2} = 4.5$ TeV.

5.1 Case with UGMs

In the SPM paper, Martin has plotted out sample spectra for two cases, one with unified gaugino masses (UGM) and one with non-unified gaugino masses (NUGM). For the case of UGM, he shows sparticle mass spectra vs. $m_{1/2}$ for $m_0 = m_{1/2}$ and also for $m_0 = 2.5m_{1/2}$, with $\tan\beta = 15$ and with $b = m_{1/2}^2$, where A_0 and μ are solved for. For the $m_0 = m_{1/2}$ case, he always finds a right selectron as the LSP (as do we), so that either additional R -parity violating interactions or lighter DM particles (such as axino) are needed to avoid charged stable relics from the early universe. In the case of $m_0 \gtrsim 2.5m_{1/2}$, then the bino can become LSP. In Fig. 13, we reproduce these results for the case of $m_0 = 2.5m_{1/2}$. The region between the pink shaded boundaries has $123 \text{ GeV} < m_h < 127 \text{ GeV}$ (as computed here using FeynHiggs [43]). Typically, in such cases with heavy sparticles in the multi-TeV range and a bino as the LSP, the thermally-produced neutralino relic density $\Omega_\chi h^2 \gg 0.12$. However, from Fig. 13 we do see that since slepton masses are very nearly equal to $m(\text{bino})$, then coannihilation is available to reproduce the measured DM relic density. We also see that the higgsino mass $\simeq \mu$ is very large, varying from $\sim 5 - 10$ TeV over the range of $m_{1/2}$ shown. This would make the model very unnatural under the conservative Δ_{EW} measure. However, the point here is that a mechanism is now present to drive the combination $m_{H_u}^2 + \mu^2$ to small values, thus potentially ameliorating the LHP.

Since we have now arrived at acceptable spectra for the case of scalar sequestering in the SPM scheme, we next want to check whether it really solves the LHP. In Fig. 14, we compute in frame *a*) the top five signed contributions to the naturalness measure Δ_{EW} . The largest

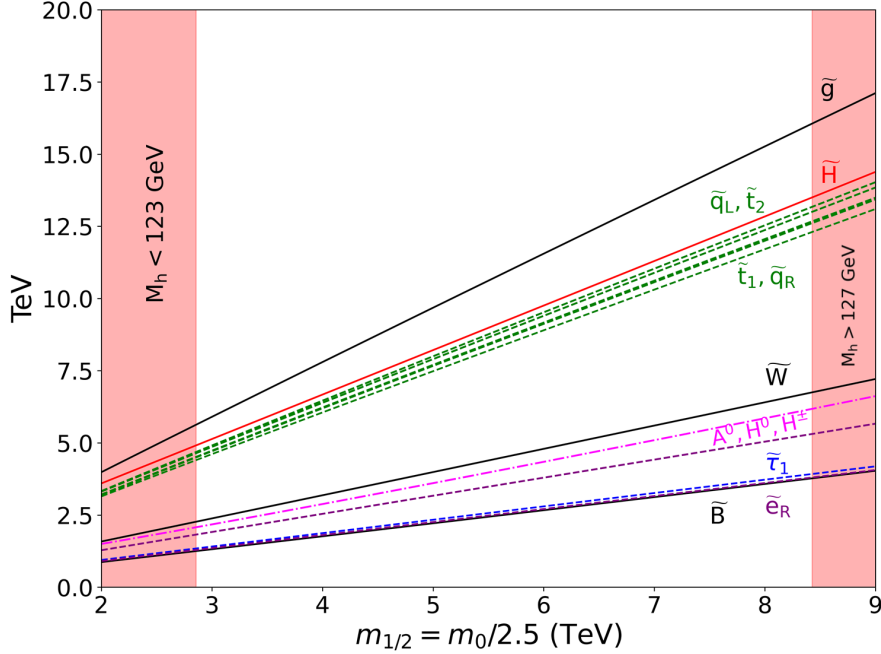


Figure 13: Sparticle masses vs. $m_{1/2}$ in the SPM UGM case with $m_{1/2} = m_0/2.5$.

contributions come from μ and m_{H_u} (*weak*), which are seen here as the blue and red curves. These lie in the $\sim 10^4$ range in magnitude, making the model highly finetuned under Δ_{EW} . In frame *b*), we define a revised finetuning measure Δ'_{EW} , which is the same as Δ_{EW} except that now $m_{H_u}^2 + \mu^2$ and $m_{H_d}^2 + \mu^2$ are combined into single entities since they are now *dependent* (due to the CFT running above $Q = M_{int}$). In frame *b*), we see the top five contributions to Δ'_{EW} . In this case, the $\Sigma_u^u(\tilde{t}_{1,2})$ terms and $\hat{m}_{H_u}^2$ terms are largest, typically of order $\sim 10^3$. Thus, we find that although the SPM scheme in the UGM case has reduced finetuning, it is still found to be highly finetuned, mainly due to the large lightly-mixed top-squark masses contributing to the radiative corrections $\Sigma_u^u(\tilde{t}_{1,2})$.

5.2 Case with NUGM

Along with the UGM case, SPM also considers the case with NUGMs. This case is motivated by obtaining a large stop mixing element A_t which can enhance $m_h \rightarrow 125$ GeV via maximal stop mixing rather than too large of stop masses. This can be achieved with $M_3 \ll M_2$ while adjusting M_1 so that the bino remains as the LSP. In Fig. 15, we show the weak scale sparticle mass spectra in the SPM scheme with NUGMs. We plot vs. m_0 where $M_3 = 1.2$ TeV, $M_2 = 4$ TeV, and $M_1 = 2$ TeV (all M_i defined at $Q = m_{GUT}$). Our calculations match well with the results of SPM. From the plot, we see that for low m_0 we still get a slepton as the LSP (this time, it is the τ -slepton $\tilde{\tau}_1$). For higher values of m_0 , then sfermion masses increase as expected and for $m_0 \gtrsim 6$ TeV one obtains $m_{\tilde{\ell}} \gtrsim m(\text{bino})$ and so we get a bino as the LSP. Also, with $M_3(m_{GUT})$ only 1.2 TeV, then squarks and sleptons are much lighter than in Fig.

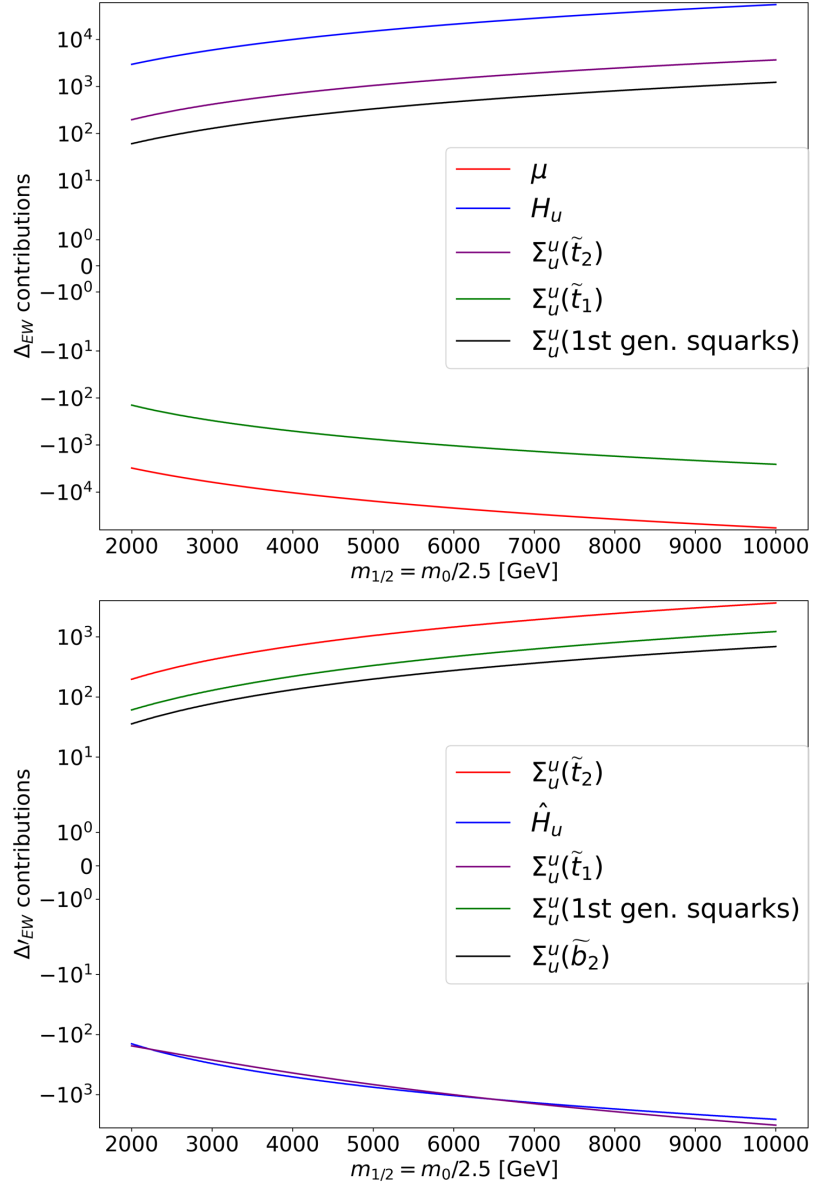


Figure 14: Top five signed contributions to a) Δ_{EW} and b) Δ'_{EW} for the UGM spectra with $m_0 = 2.5m_{1/2}$.

13. With large stop mixing, then $m_h \sim 125$ GeV with not-too-heavy of stops and a chance for naturalness. The higgsinos are heavy and lie near $|\mu| \simeq m_{\tilde{H}} \sim 2.3$ TeV.

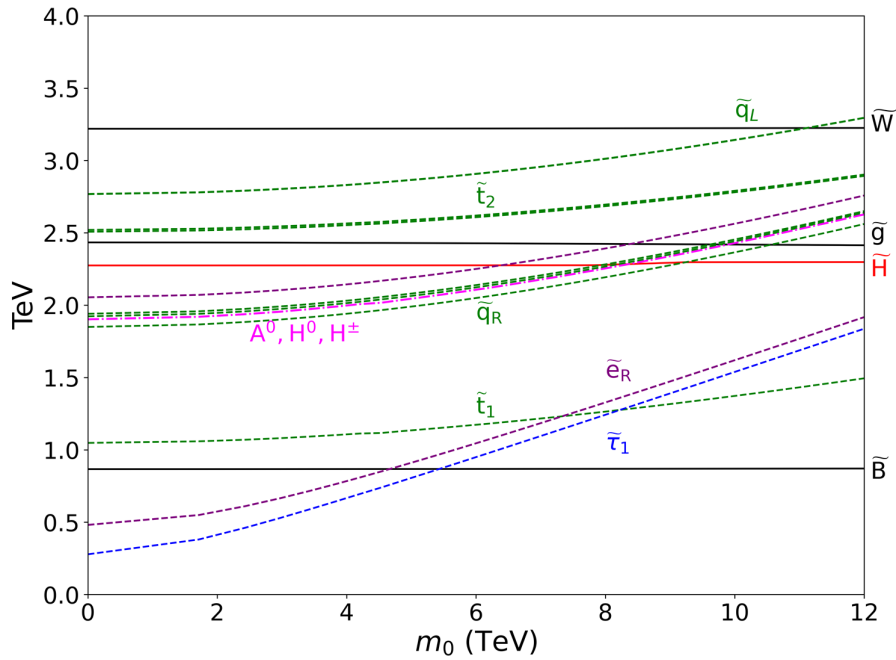


Figure 15: Sparticle and Higgs masses vs. m_0 in the SPM scheme with NUGM where $M_1 = 2$ TeV, $M_2 = 4$ TeV, and $M_3 = 1.2$ TeV, with $b = (2 \text{ TeV})^2$, $\tan \beta = 15$ and $\mu > 0$.

In Fig. 16 we compute the top five signed contributions to the finetuning measures *a)* Δ_{EW} and *b)* Δ'_{EW} for the same parameters as in Fig. 15. From frame *a)*, we see that the m_{H_u} and μ contributions to Δ_{EW} are opposite sign but with absolute values $\sim 10^3$ so that the spectra are finetuned under Δ_{EW} . However, the SS of $m_{H_{u,d}}^2 + \mu^2$ means these quantities are no longer independent and instead Δ'_{EW} should be used. From frame *b)*, we see the top five contributions to Δ'_{EW} are typically of order ~ 10 : thus, this case of the SPM scheme with NUGMs seems natural even with higgsino masses of ~ 2.3 TeV. (The breaks in the curves of frame *b)* occur due to different contributions to Eq. 1 vying to be within the top five.)

6 Conclusions

Supersymmetric models with $m_h \sim 125$ GeV which obey LHC search constraints but have low Δ_{EW} qualify as permitting a SUSY solution to the GHP while avoiding the LHP: they are electroweak natural and are typified by the presence of light higgsinos with mass $m_{\tilde{H}} \lesssim 350$ GeV. Such light higgsinos are actively being searched for by ATLAS and CMS and indeed both experiments have some small excesses in the OSDLJMET signal channels. However, here we have investigated numerically the proposition whether hidden sector scalar sequestering can yield a solution to the LHP even with large $\mu \gg 350$ GeV. The key element is to assume a nearly

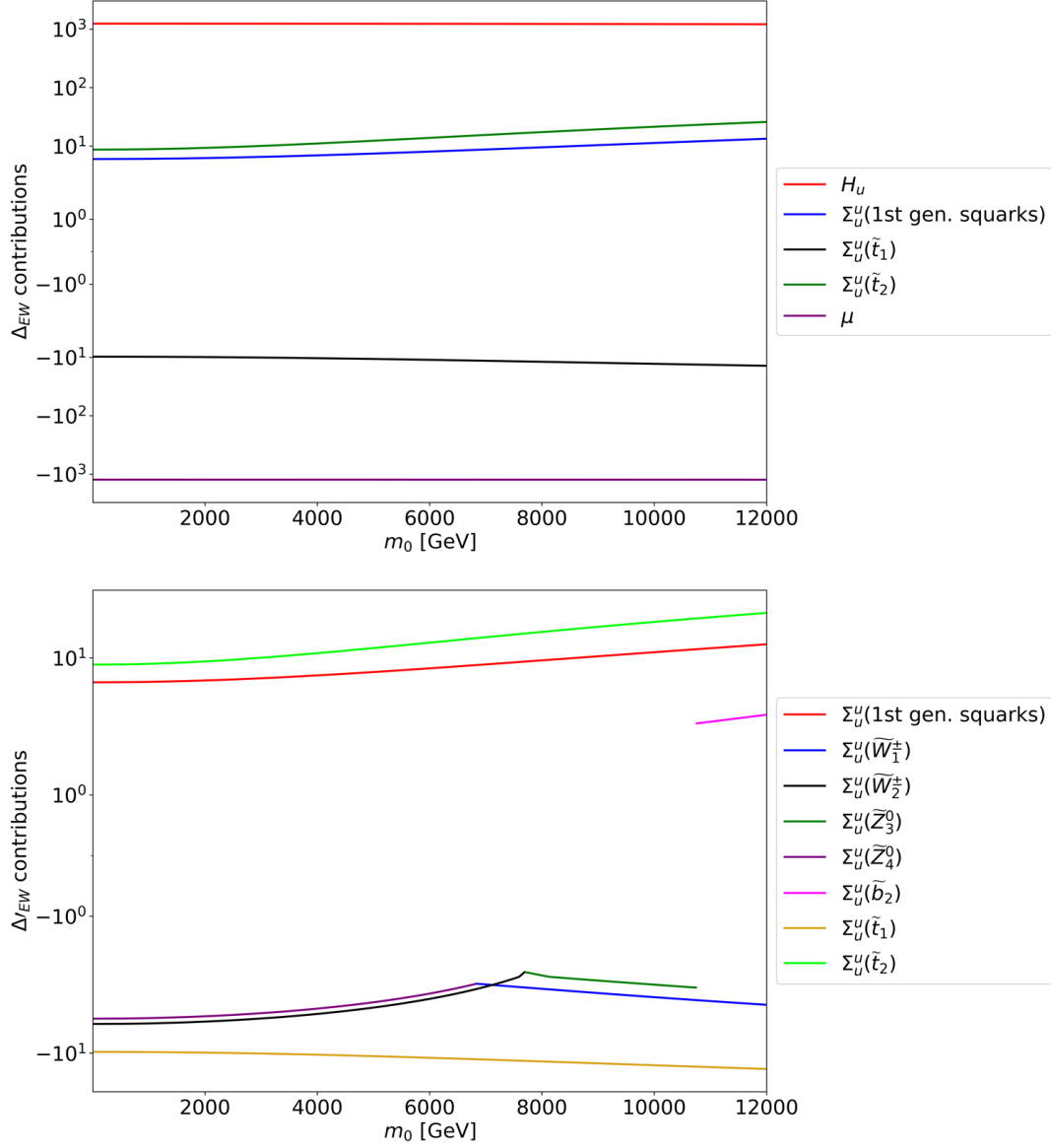


Figure 16: Top five signed contributions to a) Δ_{EW} and b) Δ'_{EW} vs. m_0 for the SPM scheme with NUGM where $M_1 = 2$ TeV, $M_2 = 4$ TeV, and $M_3 = 1.2$ TeV, with $b = (2 \text{ TeV})^2$ and $\tan \beta = 15$.

superconformal hidden sector coupled to the visible sector which leads to driving scalar masses, the $B\mu$ term and the Higgs combinations $m_{H_{u,d}}^2 + \mu^2 \rightarrow 0$ at some intermediate scale where the conformal symmetry is broken and the hidden sector is integrated out. A key ingredient is that the SUSY μ parameter is generated via the GM mechanism. In such a situation, then HS dynamics pushes $m_{H_{u,d}}^2 \sim -\mu^2$ so these quantities are no longer independent. Then a revised naturalness measure Δ'_{EW} must be used where the now dependent terms $m_{H_{u,d}}^2$ and μ^2 are combined.

We investigated two schemes.

- The strong scalar sequestering where scalar masses, $B\mu$ and Higgs combinations are driven to (nearly) zero at the intermediate scale (PRS scheme). This scheme has trouble developing appropriate electroweak symmetry breaking; and when it does, it develops a slepton as the LSP. Via thorough scans of parameter space, with both UGMs and NUGMs, we find no viable spectra with appropriate EWSB but without a slepton as the LSP. Some of the problematic slepton LSPs can be avoided by introducing new sparticle or interactions which allow one to evade cosmological constraints on charged stable relics from the Big Bang.
- The second scheme labeled as SPM introduces moderate scalar sequestering with non-negligible MSSM running so that scalar masses, $B\mu$ and Higgs combinations run to quasi-fixed points rather than zero. In the SPM scheme for UGMs, spectra with neutral stable LSPs can be found, and the finetuning can be reduced, but not eliminated. For the case of NUGMs, then $m_h \sim 125$ GeV can be found with sparticles beyond LHC bounds *and* with low EW finetuning as found from the Δ'_{EW} measure. The latter spectra can have rather heavy higgsinos since the sequestering leads to non-independent Higgs soft terms and the μ term. Determining the consequences of the viable SPM scheme with NUGMs at colliding beam experiments is a topic for future work.

Acknowledgements

This material is based upon work supported by the U.S. Department of Energy, Office of Science, Office of Basic Energy Sciences Energy Frontier Research Centers program under Award Number DE-SC-0009956. VB gratefully acknowledges support from the William F. Vilas estate.

References

- [1] H. Baer, X. Tata, Weak scale supersymmetry: From superfields to scattering events, Cambridge University Press, 2006.
- [2] H. K. Dreiner, H. E. Haber, S. P. Martin, From Spinors to Supersymmetry, Cambridge University Press, Cambridge, UK, 2023. doi:10.1017/9781139049740.
- [3] A. Canepa, Searches for Supersymmetry at the Large Hadron Collider, Rev. Phys. 4 (2019) 100033. doi:10.1016/j.revip.2019.100033.

- [4] M. Dine, Naturalness Under Stress, *Ann. Rev. Nucl. Part. Sci.* 65 (2015) 43–62. [arXiv:1501.01035](#), [doi:10.1146/annurev-nucl-102014-022053](#).
- [5] H. Baer, V. Barger, P. Huang, D. Mickelson, A. Mustafayev, X. Tata, Radiative natural supersymmetry: Reconciling electroweak fine-tuning and the Higgs boson mass, *Phys. Rev. D* 87 (11) (2013) 115028. [arXiv:1212.2655](#), [doi:10.1103/PhysRevD.87.115028](#).
- [6] H. Baer, V. Barger, D. Martinez, Comparison of SUSY spectra generators for natural SUSY and string landscape predictions, *Eur. Phys. J. C* 82 (2) (2022) 172. [arXiv:2111.03096](#), [doi:10.1140/epjc/s10052-022-10141-2](#).
- [7] H. Baer, V. Barger, D. Martinez, S. Salam, Practical naturalness and its implications for weak scale supersymmetry, *Phys. Rev. D* 108 (3) (2023) 035050. [arXiv:2305.16125](#), [doi:10.1103/PhysRevD.108.035050](#).
- [8] H. Baer, V. Barger, P. Huang, A. Mustafayev, X. Tata, Radiative natural SUSY with a 125 GeV Higgs boson, *Phys. Rev. Lett.* 109 (2012) 161802. [arXiv:1207.3343](#), [doi:10.1103/PhysRevLett.109.161802](#).
- [9] H. Baer, V. Barger, P. Huang, Hidden SUSY at the LHC: the light higgsino-world scenario and the role of a lepton collider, *JHEP* 11 (2011) 031. [arXiv:1107.5581](#), [doi:10.1007/JHEP11\(2011\)031](#).
- [10] H. Baer, V. Barger, S. Salam, D. Sengupta, X. Tata, The LHC higgsino discovery plane for present and future SUSY searches, *Phys. Lett. B* 810 (2020) 135777. [arXiv:2007.09252](#), [doi:10.1016/j.physletb.2020.135777](#).
- [11] H. Baer, V. Barger, D. Sengupta, X. Tata, New angular and other cuts to improve the Higgsino signal at the LHC, *Phys. Rev. D* 105 (9) (2022) 095017. [arXiv:2109.14030](#), [doi:10.1103/PhysRevD.105.095017](#).
- [12] G. Aad, et al., Searches for electroweak production of supersymmetric particles with compressed mass spectra in $\sqrt{s} = 13$ TeV pp collisions with the ATLAS detector, *Phys. Rev. D* 101 (5) (2020) 052005. [arXiv:1911.12606](#), [doi:10.1103/PhysRevD.101.052005](#).
- [13] A. Tumasyan, et al., Search for supersymmetry in final states with two or three soft leptons and missing transverse momentum in proton-proton collisions at $\sqrt{s} = 13$ TeV, *JHEP* 04 (2022) 091. [arXiv:2111.06296](#), [doi:10.1007/JHEP04\(2022\)091](#).
- [14] Z. Han, G. D. Kribs, A. Martin, A. Menon, Hunting quasidegenerate Higgsinos, *Phys. Rev. D* 89 (7) (2014) 075007. [arXiv:1401.1235](#), [doi:10.1103/PhysRevD.89.075007](#).
- [15] H. Baer, A. Mustafayev, X. Tata, Monojet plus soft dilepton signal from light higgsino pair production at LHC14, *Phys. Rev. D* 90 (11) (2014) 115007. [arXiv:1409.7058](#), [doi:10.1103/PhysRevD.90.115007](#).
- [16] H. Murayama, Y. Nomura, D. Poland, More visible effects of the hidden sector, *Phys. Rev. D* 77 (2008) 015005. [arXiv:0709.0775](#), [doi:10.1103/PhysRevD.77.015005](#).

- [17] G. Perez, T. S. Roy, M. Schmaltz, Phenomenology of SUSY with scalar sequestering, *Phys. Rev. D* 79 (2009) 095016. [arXiv:0811.3206](#), [doi:10.1103/PhysRevD.79.095016](#).
- [18] H. D. Kim, J.-H. Kim, Higgs Phenomenology of Scalar Sequestering, *JHEP* 05 (2009) 040. [arXiv:0903.0025](#), [doi:10.1088/1126-6708/2009/05/040](#).
- [19] S. P. Martin, Quasifixed points from scalar sequestering and the little hierarchy problem in supersymmetry, *Phys. Rev. D* 97 (3) (2018) 035006. [arXiv:1712.05806](#), [doi:10.1103/PhysRevD.97.035006](#).
- [20] M. Luty, R. Sundrum, Anomaly mediated supersymmetry breaking in four-dimensions, naturally, *Phys. Rev. D* 67 (2000) 045007. [arXiv:hep-th/0111231](#), [doi:10.1103/PhysRevD.67.045007](#).
- [21] L. Randall, R. Sundrum, Out of this world supersymmetry breaking, *Nucl. Phys. B* 557 (1999) 79–118. [arXiv:hep-th/9810155](#), [doi:10.1016/S0550-3213\(99\)00359-4](#).
- [22] G. F. Giudice, M. A. Luty, H. Murayama, R. Rattazzi, Gaugino mass without singlets, *JHEP* 12 (1998) 027. [arXiv:hep-ph/9810442](#), [doi:10.1088/1126-6708/1998/12/027](#).
- [23] A. Anisimov, M. Dine, M. Graesser, S. D. Thomas, Brane world SUSY breaking, *Phys. Rev. D* 65 (2002) 105011. [arXiv:hep-th/0111235](#), [doi:10.1103/PhysRevD.65.105011](#).
- [24] M. Dine, P. J. Fox, E. Gorbatov, Y. Shadmi, Y. Shirman, S. D. Thomas, Visible effects of the hidden sector, *Phys. Rev. D* 70 (2004) 045023. [arXiv:hep-ph/0405159](#), [doi:10.1103/PhysRevD.70.045023](#).
- [25] N. J. Craig, D. Green, On the Phenomenology of Strongly Coupled Hidden Sectors, *JHEP* 09 (2009) 113. [arXiv:0905.4088](#), [doi:10.1088/1126-6708/2009/09/113](#).
- [26] G. F. Giudice, R. Rattazzi, Theories with gauge mediated supersymmetry breaking, *Phys. Rept.* 322 (1999) 419–499. [arXiv:hep-ph/9801271](#), [doi:10.1016/S0370-1573\(99\)00042-3](#).
- [27] T. S. Roy, M. Schmaltz, Hidden solution to the $\mu/B\mu$ problem in gauge mediation, *Phys. Rev. D* 77 (2008) 095008. [arXiv:0708.3593](#), [doi:10.1103/PhysRevD.77.095008](#).
- [28] G. F. Giudice, A. Masiero, A Natural Solution to the μ Problem in Supergravity Theories, *Phys. Lett. B* 206 (1988) 480–484. [doi:10.1016/0370-2693\(88\)91613-9](#).
- [29] K. J. Bae, H. Baer, V. Barger, D. Sengupta, Revisiting the SUSY μ problem and its solutions in the LHC era, *Phys. Rev. D* 99 (11) (2019) 115027. [arXiv:1902.10748](#), [doi:10.1103/PhysRevD.99.115027](#).
- [30] V. D. Barger, G. F. Giudice, T. Han, Some New Aspects of Supersymmetry R-Parity Violating Interactions, *Phys. Rev. D* 40 (1989) 2987. [doi:10.1103/PhysRevD.40.2987](#).

- [31] H. K. Dreiner, An Introduction to explicit R-parity violation, *Adv. Ser. Direct. High Energy Phys.* 21 (2010) 565–583. [arXiv:hep-ph/9707435](#), [doi:10.1142/9789814307505_0017](#).
- [32] K.-Y. Choi, L. Covi, J. E. Kim, L. Roszkowski, Axino Cold Dark Matter Revisited, *JHEP* 04 (2012) 106. [arXiv:1108.2282](#), [doi:10.1007/JHEP04\(2012\)106](#).
- [33] H. Baer, V. Barger, D. Mickelson, M. Padeffke-Kirkland, SUSY models under siege: LHC constraints and electroweak fine-tuning, *Phys. Rev. D* 89 (11) (2014) 115019. [arXiv:1404.2277](#), [doi:10.1103/PhysRevD.89.115019](#).
- [34] M. Carena, H. E. Haber, Higgs Boson Theory and Phenomenology, *Prog. Part. Nucl. Phys.* 50 (2003) 63–152. [arXiv:hep-ph/0208209](#), [doi:10.1016/S0146-6410\(02\)00177-1](#).
- [35] S. P. Martin, M. T. Vaughn, Two-loop renormalization group equations for soft supersymmetry-breaking couplings, *Phys. Rev. D* 50 (1994) 2282–2292. [doi:10.1103/PhysRevD.50.2282](#).
- [36] B. Allanach, SOFTSUSY: A program for calculating supersymmetric spectra, *Computer Physics Communications* 143 (3) (2002) 305–331. [doi:10.1016/s0010-4655\(01\)00460-x](#).
- [37] A. Buckley, PySLHA: a Pythonic interface to SUSY Les Houches Accord data (2015). [arXiv:1305.4194](#).
- [38] M. Srednicki, K. A. Olive, J. Silk, High-Energy Neutrinos from the Sun and Cold Dark Matter, *Nucl. Phys. B* 279 (1987) 804–823. [doi:10.1016/0550-3213\(87\)90020-4](#).
- [39] J. Aalbers, et al., First Dark Matter Search Results from the LUX-ZEPLIN (LZ) Experiment, *Phys. Rev. Lett.* 131 (4) (2023) 041002. [arXiv:2207.03764](#), [doi:10.1103/PhysRevLett.131.041002](#).
- [40] D. Poland, D. Simmons-Duffin, A. Vichi, Carving Out the Space of 4D CFTs, *JHEP* 05 (2012) 110. [arXiv:1109.5176](#), [doi:10.1007/JHEP05\(2012\)110](#).
- [41] D. Poland, A. Stergiou, Exploring the Minimal 4D $\mathcal{N} = 1$ SCFT, *JHEP* 12 (2015) 121. [arXiv:1509.06368](#), [doi:10.1007/JHEP12\(2015\)121](#).
- [42] D. Green, D. Shih, Bounds on SCFTs from Conformal Perturbation Theory, *JHEP* 09 (2012) 026. [arXiv:1203.5129](#), [doi:10.1007/JHEP09\(2012\)026](#).
- [43] T. Hahn, S. Heinemeyer, W. Hollik, H. Rzehak, G. Weiglein, FeynHiggs: A program for the calculation of MSSM Higgs-boson observables - Version 2.6.5, *Comput. Phys. Commun.* 180 (2009) 1426–1427. [doi:10.1016/j.cpc.2009.02.014](#).